Supplementary Material

3D analysis of equally X-ray attenuating mineralogical phases utilizing a correlative tomographic workflow across multiple length scales

Silvan Englisch[1], Ralf Ditscherlein[2], Tom Kirstein[3], Leonard Hansen[4], Orkun Furat[3], Dominik Drobek[1], Thomas Leißner[2], Benjamin Apeleo Zubiri[1,*], Alfred P. Weber[4], Volker Schmidt[3], Urs A. Peuker[2], and Erdmann Spiecker[1,*]

[1]Institute of Micro- and Nanostructure Research (IMN) & Center for Nanoanalysis and Electron Microscopy (CENEM), Interdisciplinary Center for Nanostructured Films (IZNF), Friedrich-Alexander-Universität Erlangen-Nürnberg (FAU), Cauerstr. 3, 91058 Erlangen, Germany

[2]Institute of Mechanical Process Engineering and Mineral Processing, Technische Universität Bergakademie Freiberg, 09599 Freiberg, Germany

[3]Institute of Stochastics, Ulm University, 89069 Ulm, Germany

[4]Institute of Particle Technology, Clausthal University of Technology, 38678 Clausthal-Zellerfeld, Germany

[*]corresponding authors: erdmann.spiecker@fau.de, benjamin.apeleo.zubiri@fau.de

Appendix A: Particle System

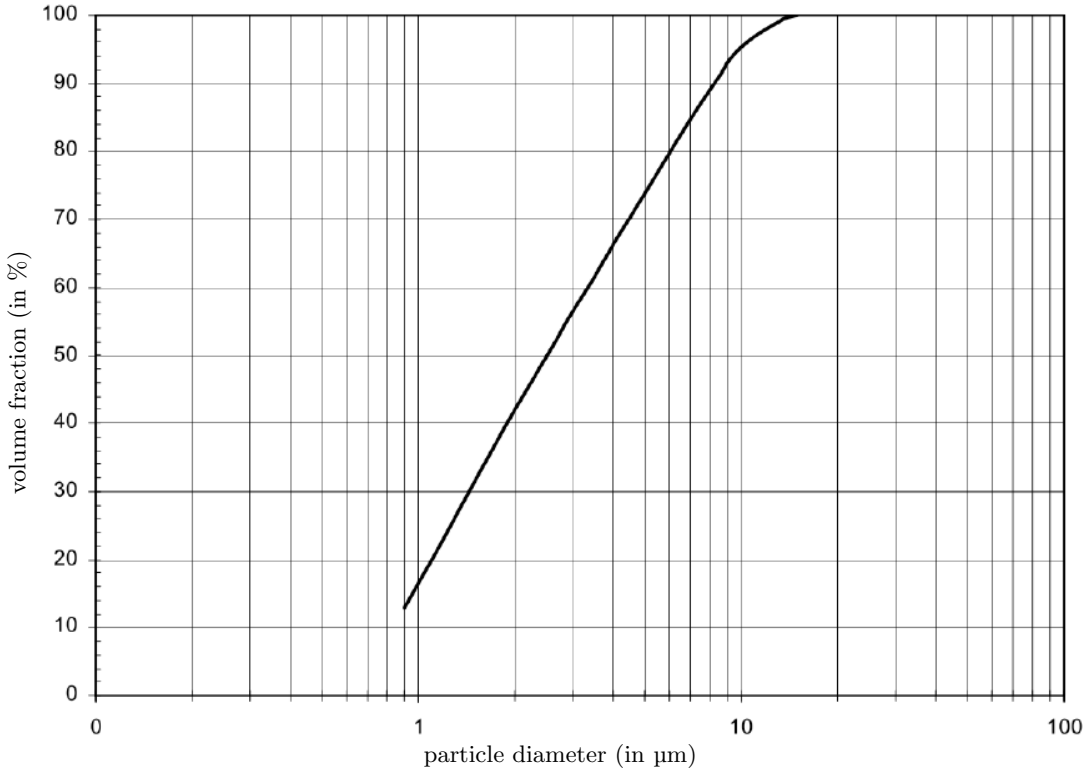

Figure S1: Cumulative distribution function of particle sizes for saxolite from manufacturer measured by laser diffraction.

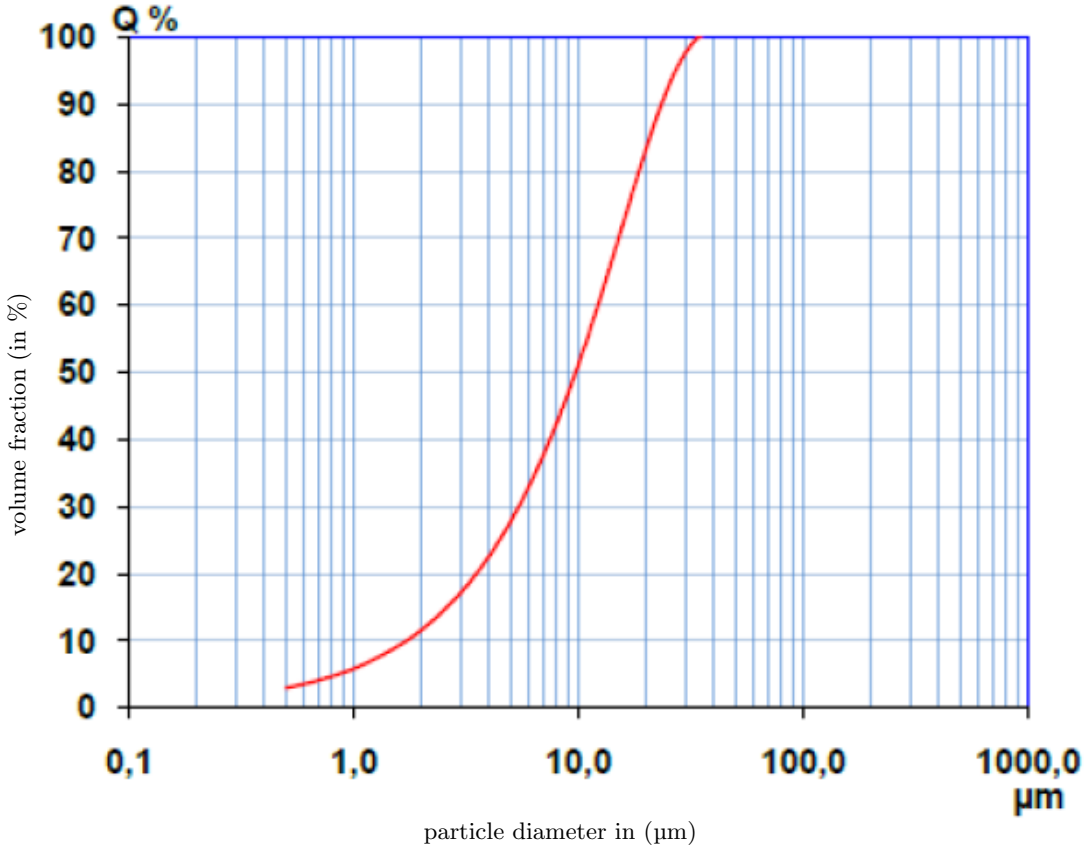

Figure S2: Cumulative distribution function of particle sizes for talcum (incl. dolomite and magnesite) from manufacturer measured by sedimentation analysis.

Table S1: Densities of both original powders in g/m^3

Saxolite	**Talcum**
2.75	2.8

Appendix B: Tomographic Measurements

Table S2: Measurement and reconstruction parameters of all 3 resolution modes - low-resolution (low-res), medium-resolution (med-res) and high-resolution (high-res); (∗) not applicable for monochromatic measurements.

parameter	**micro-CT** *low resolution*	**micro-CT** *medium resolution*	**nano-CT** *high resolution*
sample size diameter / mm	1.6	0.5	0.060
field of view (FOV) / mm	1.5	0.3	0.065
acceleration voltage / keV	80	80	5.4
electrical power / W	7	7	900
target material / –	tungsten	tungsten	chromium
source filter (Zeiss standard)	LE4	LE4	∗
exposure time / s	2	25	70
optical magnification / x	4	40	∗
number of projections	3201	3201	901
angle range / °	360	360	180
voxel size / µm	1.5	0.3	0.064
binning	2	2	1
reconstruction algorithm	FBP	FBP	SIRT
smoothing (Gauß)	0.1	0.1	–
beam hardening correction	0.05	0.05	∗

Appendix C: Laser-ablated Sample

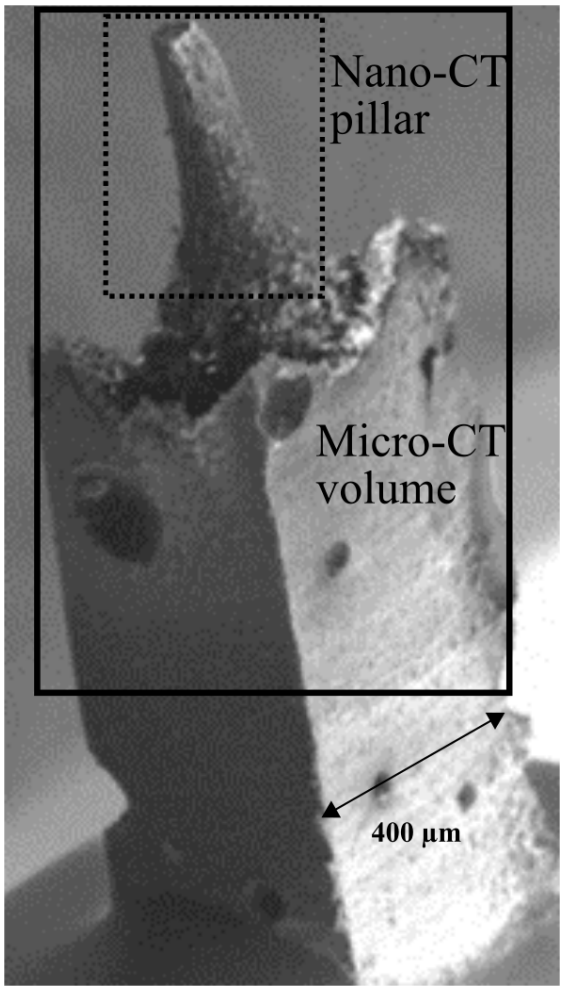

Figure S3: Laser-ablated Micro-CT sample to fit the field of view of Nano-CT.

Appendix D: 3D Segmentation

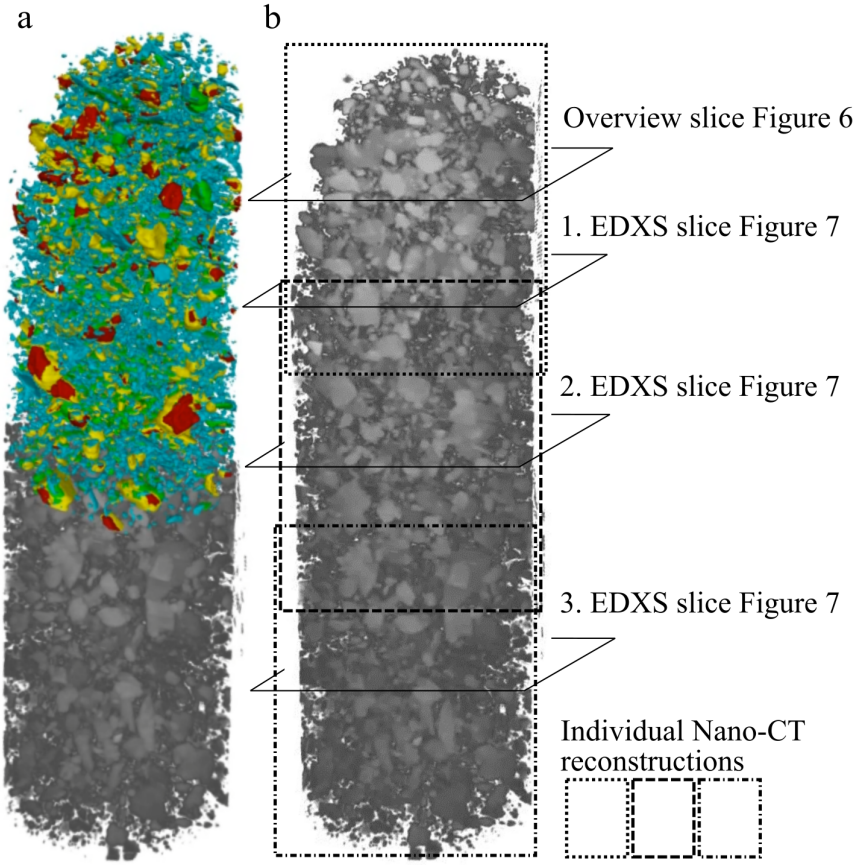

Figure S4: (a) Phase-related segmentation workflow visualized in 3D for the complete Nano-CT volume (stitched volume of three single, adjacent Nano-CT volumes). Phase-discrete segmentation side by side with gray-scale image. (b) Indicated positions of the single Nano-CT volumes in the stitched Nano-CT volume and slice positions of the acquired EDXS maps.

Appendix E: Phase-wise and Particle-wise Segmentation

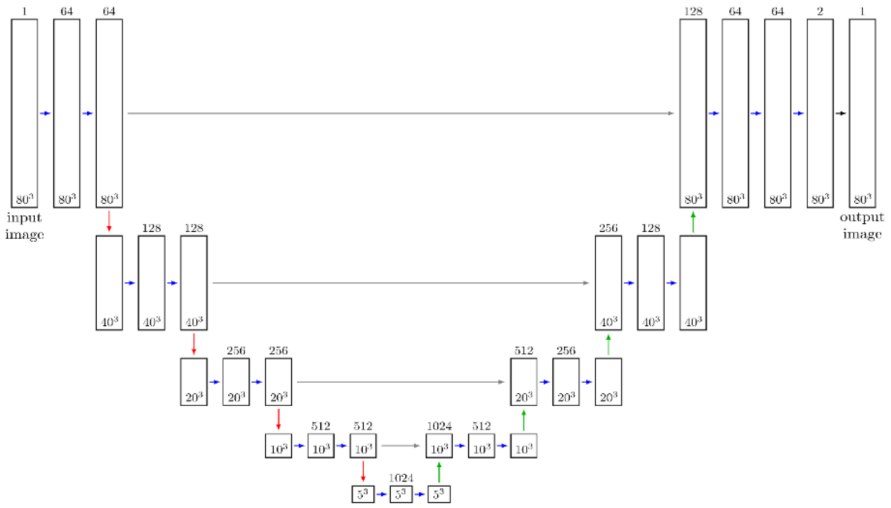

Figure S5: U-net architecture.

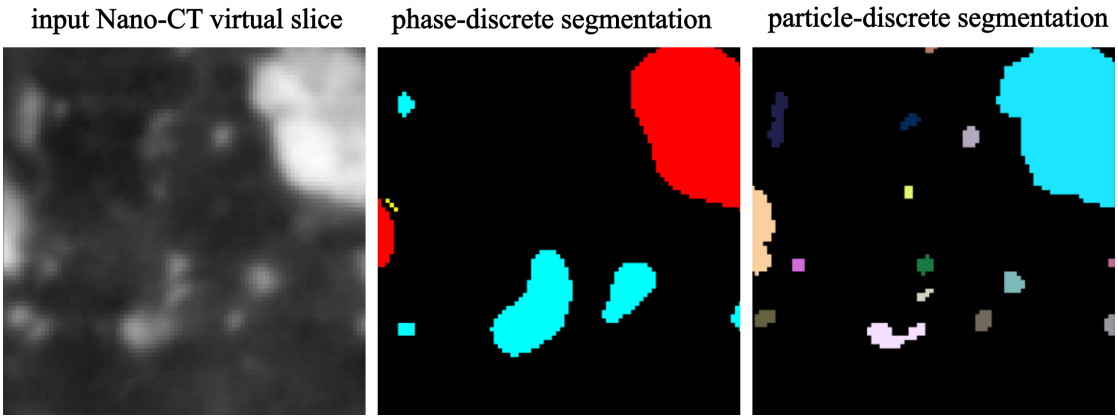

Figure S6: Results of phase-discrete and particle-discrete segmentation algorithms applied to the Nano-CT reconstructions, visualized for an exemplary colorized slice.

Appendix F: Further Grain over Particle Volume Maps

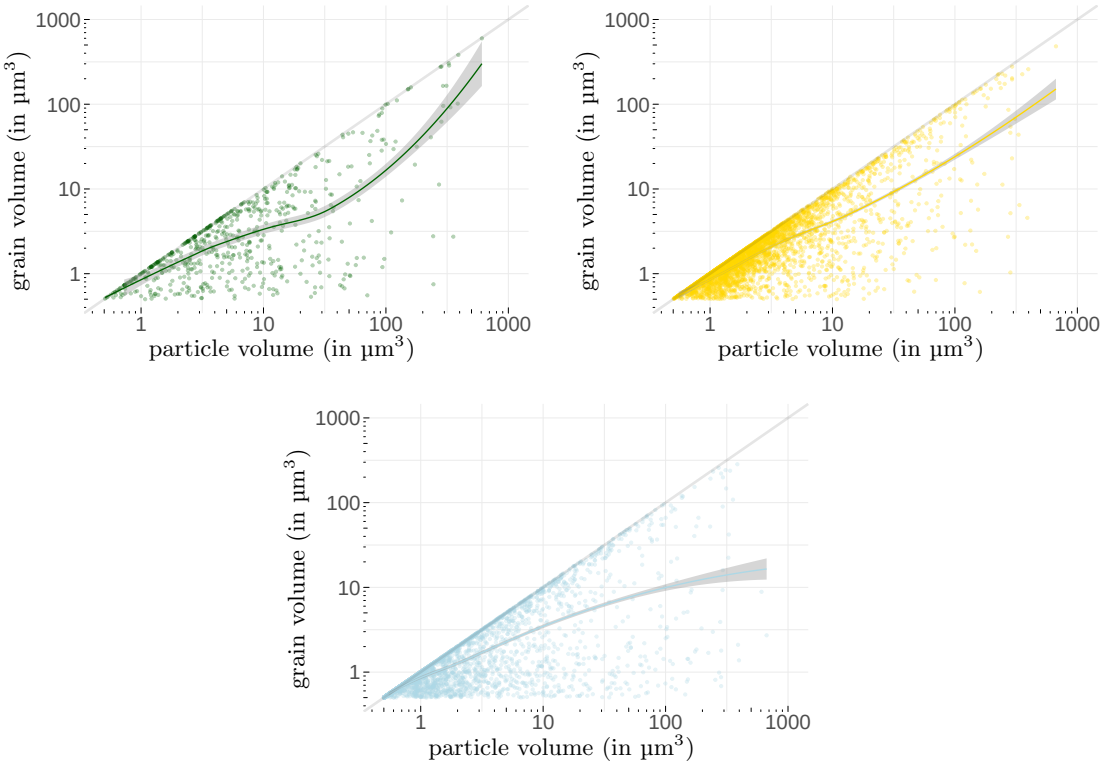

Figure S7: Grain over particle volume map targeting magnesite (green), dolomite (yellow) and talcum (blue). The colored curves illustrate the mean grain volume for a given particle volume, whereas the gray shadowing indicates the corresponding error bars.